Modeled response of the East China Sea shelf water to wind forcing

Moon, Jae-Hong
Jet Propulsion Laboratory, California Institute of Technology, Pasadena, California, USA

Hirose, Naoki
Research Institute for Applied Mechanics, Kyushu University

https://doi.org/10.15017/27129

出版情報：九州大学応用力学研究所所報. 143, pp.7-17, 2012-09. Research Institute for Applied Mechanics, Kyushu University
バージョン：
権利関係：

Modeled response of the East China Sea shelf water to wind forcing

Jae-Hong Moon[1*] and Naoki Hirose[2]

E-mail of corresponding author: *Jae-Hong.Moon@jpl.nasa.gov*

(Received July 7, 2012)

Abstract

Seasonal variation of the East China Sea (ECS) shelf water in response to wind forcing is examined using a northwestern Pacific model. By comparison of the simulations with wind and without wind conditions, in winter strong northeasterly wind significantly weakens the Taiwan Warm Current entering the ECS shelf through the Taiwan Strait, and plays a role in intensifying onshore Kuroshio intrusion northeast of Taiwan. Contribution of the Taiwan Warm Current water and Kuroshio water to the property of ECS shelf water is estimated by releasing two separate tracers into the model. With wind forcing the tracer contribution from the Taiwan Strait shows a minimum in winter and maximum in summer, while that from the Kuroshio has an opposite seasonal contribution to that from the Taiwan Strait. Therefore, origin of the material passing through the Korea/Tsushima Strait varies seasonally. When wind forcing is not applied to the model, however, the seasonal variability almost disappears, implying that contributions from the tracers are direct consequences of the seasonal variation of the Taiwan Warm Current and onshore Kuroshio intrusion due to wind forcing. Furthermore, the shelf water changes seasonally regardless of Ekman transport across the ECS shelf break. This suggests that the variability of the shelf water could be controlled by changes in the strength of the Taiwan Warm Current driven by wind over the strait, which appear to block the Kuroshio water on the shelf and thus prevent the onshore Kuroshio intrusion northeast of Taiwan.

Key words : *Seasonal variation, East China Sea shelf water, wind forcing, Taiwan Warm Current, onshore Kuroshio intrusion, tracer concentration*

1. Introduction

The East China Seas (ECS) are a marginal sea of the northwestern Pacific Ocean, surrounded by Korea, China and the chain of Ryukyu Islands. Seasonal circulation in the ECS depends closely on the broad and shallow continental shelf, Kuroshio as a strong western boundary current, Taiwan Warm Current, and atmospheric conditions.

The Kuroshio, entering the ECS shelf at the northeast of Taiwan, flows northeastward along the continental shelf break of the ECS. The onshore Kuroshio intrusion is a well-known phenomenon observed by several researchers (Liu et al., 1992; Chern and Wang, 1992; Tang et al., 1999). Chern and Wang (1992) suggested that seasonal variation of the onshore Kuroshio intrusion is related with the inflow from through the Taiwan Strait. Recently, realistic numerical model approaches have become available for the evaluation of this intrusion (Guo et al, 2006; Isobe and Beardsley, 2006; Lee and Matsuno, 2007). Guo et al. (2006) estimated that the seasonal onshore Kuroshio transport show an increase from autumn to winter with a minimum in summer. They also suggested that its seasonal variation is primarily controlled by the Ekman transport across the shelf break of the ECS.

The transport through the Taiwan Strait has a remarkable seasonal variation with a minimum in winter and maximum in summer (Jan et al., 2002; Jan and Chao, 2003; Wang et al., 2003). Wang et al. (2003) estimated that the throughflow transport in the Taiwan Strait has a minimum of 0.9 Sv in winter and a maximum of 2.7 Sv in summer, using the shipboard ADCP for 2.5 years and along-strait wind data. Recent current data by Lin et al. (2005) demonstrated that the northeastward Taiwan Warm Current considerably weakens when the northeasterly wind strengthens over the strait.

From these variations, we can conjecture that the contribution of the Taiwan Warm Current water and Kuroshio water to the ECS shelf water varies seasonally. The origin of the material passing through the Korea/Tsushima

*1 Jet Propulsion Laboratory, California Institute of Technology, Pasadena, California, USA.

*2 Research Institute for Applied Mechanics, Kyushu University

Strait may be also changed seasonally. If so, how are the properties of the ECS shelf water changed seasonally? And, what makes the seasonal phenomena?

Seasonal variability in the ECS is large because of the shallow shelf region and climate conditions related to the winter and summer monsoons. Wind forcing could be one of the major factors driving the seasonal water mass distribution and circulation in the ECS. Many researchers have studied the effect of wind in the ECS using a local sea models (Yanagi and Takahashi, 1993; Jacobs et al., 2000; Lee and Matsuno, 2007). In general, the results of a local sea model depend closely on the artificial boundary conditions along the open boundary, where the vertical structures of current as well as their temporal variations are usually unknown (Guo et al., 2006). In particular, the ECS environment is strongly affected by the inflows through the Taiwan Strait and the Kuroshio and the outflows through the Korea/Tsushima and Tokara Straits as the open boundary conditions.

For instance, using a local ECS model Jacobs et al. (2000) examined the contributions of the Kuroshio and the Taiwan Warm Current to the ECS environment. However, their model has several unrealistic components, such as the artificially closed southeastern boundary and fixed open boundaries. The closed southeastern boundary excludes transport due to the Kuroshio recirculation gyres. In addition to this, the fixed Taiwan Strait velocity blocks the southward Chinese coastal current in winter and forces to turn to the northeastward joining the Taiwan Warm Current. Thus, the transport on the shelf can be overestimated. It is difficult to diagnose the physical process associated with the open boundaries because the wind forcing affects the inflow and outflow conditions in the ECS.

In this study we use a northwestern Pacific circulation model (Moon et al., 2009) to develop insight on how the ECS shelf region responds to wind forcing. The northwestern Pacific model can be a solution to the boundary problems in the local ECS model mentioned above. The numerical model setup and conditions are described in the next section. Responses of the water mass distribution and circulation in the ECS to wind forcing are presented in section 3 and 4, respectively. In section 5 a passive tracer experiment is conducted to understand the contributions of the Taiwan Warm Current and the Kuroshio to the ECS shelf water in response to wind forcing. Then, we discuss the origin of the material passing through the Korea/Tsushima Strait and the role of the Taiwan Warm Current on the ECS shelf water in section 6. Finally, interpretations of the numerical calculations are summarized in section 7.

2. Numerical model setup and conditions

2.1 General description of model

The numerical model (RIAM Ocean Model, RIAMOM) used in this study is a three-dimensional, z-coordinate primitive equation OGCM developed by Lee (1996). The RIAMOM assumes the Boussinesq, hydrostatic balance and solves the three-dimensional, non-linear, free-surface, primitive equations. The finite differencing is based on Arakawa's B-grid system horizontally and allows partial stepping for the bottom cell vertically (Adcroft et al., 1997). Momentum conservation is implemented by a generalized Arakawa scheme (Ishizaki and Moti, 1999). Momentum diffusion is given by a fourth-order difference. The so-called *slant advection* effect (Takano, 1978) is adopted to correctly represent the vertical advection of the horizontal momentum along the steep bottom topography. This model includes improved advection scheme for tracers, so called Modified Split QUICK (MSQ) scheme (Webb et al., 1998). The vertical coefficients of eddy viscosity and diffusivity were calculated by solving the turbulent kinetic energy equation (Noh et al., 2002). Details of the RIAMOM computational schemes are suggested by Lee (1996).

2.2 Model setup and conditions

The model region covers the northwestern Pacific marginal seas from the South China Sea to the East/Japan Sea (15-52°N, 110-148°E) with 1/6 degree horizontal resolution and 60 vertical levels. The bottom topography is extracted from a combination of two topographic data sets, ETOPO5 and SKKU (1 minute horizontal resolution; Choi et al., 2002). The model is initialized with climatological temperature and salinity obtained from GDEM (the U.S. Navy's Generalized Digital Environmental Model). This dataset has been built on the U.S. Navy's Master Oceanographic Observation Data Set (MOODS) with 8 million profiles.

For the lateral boundary conditions, the GDEM monthly mean temperature, salinity, and velocity fields of the Pacific Ocean model by You and Yoon (2004) are used to estimate climatological values of the boundaries. This climatology is used at open boundaries as external data with a nudging scheme. All climatology conditions are linearly interpolated at each model time step. One advantage of this model is that some problems concerning inflow (the Taiwan Strait and east of Taiwan) and outflow (the Korea/Tsushima and Tokara Straits) conditions in the ECS cannot be considered. Therefore, it is reasonable to use the numerical model to diagnose the physical mechanisms in these straits.

Atmospheric forcing is based on climatological data derived from the Comprehensive Ocean-Atmosphere Data Set (COADS) (Da Silva et al., 1994) and QuikSCAT wind data (obtained by CERSAT). These forcings include surface

heat and heat flux sensitivity to sea surface temperature (Barnier et al., 1995). The model heat flux appears as the sum of climatological flux and a correction term proportional to the difference between the climatological sea surface temperature and the model surface temperature.

$$Q_{net}(T_{mod}) = Q_{net}(T_{clm}) + \left(\frac{\partial Q_{net}}{\partial T}\right)(T_{clm-} - T_{mod}) \quad (1)$$

where $Q_{net}(T_{clm})$ is the climatological net heat flux, T_{clm} is the climatological sea surface temperature, and T_{mod} is the model sea surface temperature. The sea surface salinity is restored at the surface grid using the GDEM climatology data.

The model was spun up with all forces for 24 model years. After 24 years of spin-up, three numerical experiments were run for additional four years: one with wind forcing (case 1) and one without (case 2a). To discuss the role of the Taiwan Warm Current on the ECS shelf water, an additional experiment was conducted with a local wind forcing which is only applied in the Taiwan Strait region (case 2b). These operations are summarized in Table 1.

Table 1 Summary of numerical experiments

Name	Seasonal wind stress	Descriptions
Case 1	Yes	Wind is applied in entire model domain
Case 2a	No	Wind is not applied in entire model domain
Case 2b	Yes	Wind is applied only in the Taiwan Strait region

3. Response of the ECS shelf water to wind forcing

Fig. 1 shows the monthly mean temperature at 50 m depth for (a) case 1 (with wind forcing) and (b) case 2a (without wind forcing) in February and August. The observed temperature distributions are also shown in Fig. 1c for comparison. In winter a prominent difference between the cases 1 and 2a is found in the Taiwan Strait and off northeast of Taiwan. In case 1 water warmer than 20°C mainly intrudes onto the ECS shelf at the northeast of Taiwan and is distributed along the ECS shelf break (Fig. 1a). In case 2a, however, the intrusion at the northeast of Taiwan become weaker than that of case 1, while the intrusion through the Taiwan Strait is relatively strengthened (Fig. 1b). The winter distribution in case 1 rather than in case 2 is fairly consistent with the observation as shown in Fig. 1c.

Meanwhile, temperature patterns are quite similar for both cases during summertime. High-temperature water intrudes onto the shelf from the Taiwan Strait and the northeast of Taiwan and the warm water on the ECS shelf is distributed toward the Korea/Tsushima Strait (Fig. 1). Relatively cold water is also observed over the edge of the shelf northeast of Taiwan, originated from upwelling. Tang et al. (1999) demonstrated the existence of the upwelling, based on a single cruise of ship-board Acoustic Doppler Current Profiler (Sb-ADCP) in summertime. The summer temperature distribution agrees well with the observed distribution except for the cold water structure from the YS toward the northern ECS. As shown in Fig. 1c, low-temperature water in the YS expands southward toward the northern ECS as a tongue- shaped pattern in the lower layer, which is called the southward expansion of the Yellow Sea Bottom Cold Water (YSBCW, Park, 1986; Kim et al., 1991; Youn et al., 1991). However, the southward expansion of the YSBCW was not detected in the model-predicted distributions, indicating that the movement is regardless of wind conditions. This phenomenon is related to strong tidal effects in the YS as reported by Moon et al. (2009). Using a three-dimensional numerical model with M_2 tide, they suggested that the southward movement of the YSBCW in summer can be contributed by the southward tidal residual current along the western slope of the YS, which is intensified by the interaction with strong summer stratification and bottom topography.

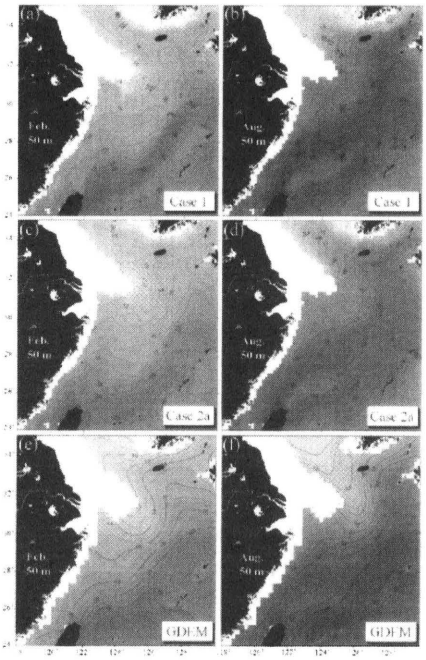

Fig. 1 Comparison of temperature distributions at 50 m depth in February and August among the results of (a, b) case 1, (c, d) case 2a and (e, f) GDEM data. Contour interval is 1°C.

4. Response of currents on the ECS shelf to wind forcing

Associated with the wind-driven changes in water mass distributions are also shown in the current distributions. As presented in Fig. 2a, for case 1 a northeastward flow is seen in the Taiwan Strait, that is, the Taiwan Warm Current, and it flows northeastward along the ECS shelf during the wintertime. A substantial portion of the Kuroshio flows northward to the northeast of Taiwan and then turns clockwise. This clockwise-turning current flows northeastward along the 200 m isobath on the continental slope of the ECS and turns southeastward to go through the Tokara Strait. The onshore Kuroshio intrusion northeast of Taiwan agrees well with the observations and numerical simulations (Qiu and Imasato, 1990; Chern and Wang, 1992; Tang et al., 2000; Guo et al., 2006; Lee and Matsuno, 2007; Hsin et al., 2008).

However, in the absence of wind forcing the Taiwan Warm Current is significantly intensified and onshore Kuroshio intrusion northeast of Taiwan is relatively weakened (left panel of Fig. 2b). The velocity difference of case 1 minus case 2a exemplifies the effect of wintertime wind on the current in this region (Fig. 3a). In winter strong southwestward anomaly flow appears in the Taiwan Strait, while a northward anomaly flow intrudes onto the shelf region shallower than 200 m off northeast of Taiwan. The northward flow across the 200 m isobath reaches its maximum of ~ 15 cm s^{-1}. The velocity difference implies that the winter wind weakens northeastward flow through the Taiwan Strait, while it intensifies onshore Kuroshio intrusion northeast of Taiwan. As a result, the winter transport through the Taiwan Strait become much larger in case 2a than in case 1 (Table 2). In winter the volume transport through the Taiwan Strait is 0.7 Sv in case 1, but that increases up to 2.4 Sv in case 2a. It supports that strong northeasterly wind primarily drives the volume transport through the Taiwan Strait in wintertime.

With wind forcing the Taiwan Warm Current is stronger in summer than in winter (right panel of Fig. 2a). The current through the Taiwan Strait flows northeastward parallel to the 50 m isobath and reaches the Kuroshio frontal area (around 30°N) and then deflects northward to the southern sea of Korea and the Korea/Tsushima Strait. A part of the Taiwan Warm Current enters a submerged river valley off the Changjiang along the 50 m isobath (Jan et al., 2002; Chang and Isobe, 2003). The Tsushima Warm Current, entering the Korea/Tsushima Strait from the ECS, becomes stronger in summer. The Kuroshio off northeast of Taiwan shifts seaward in summer, indicating that the Kuroshio intruded onto the shelf is weakened. Then the Kuroshio flows northeastward along the 200 m isobath on the shelf edge. Historical GEK (Geomagnetic ElectroKinetograph) measurements concluded that the Kuroshio off northeast of Taiwan migrates shoreward from fall to winter and seaward from spring to summer.

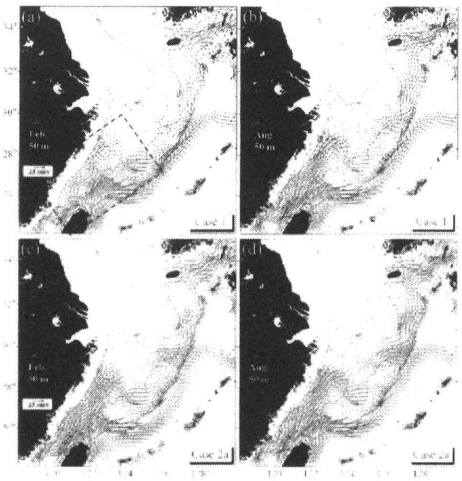

Fig. 2 Comparison of current distributions at 50 m depth in February and August between the results of (a, b) case 1 and (c, d) case 2a. Vectors in the area deeper than 200 m are rescaled by the factor of 0.25. Dashed lines indicate 50 m, 100 m and 200 m isobaths. Rotated square box is the region for the velocity difference of Fig. 3.

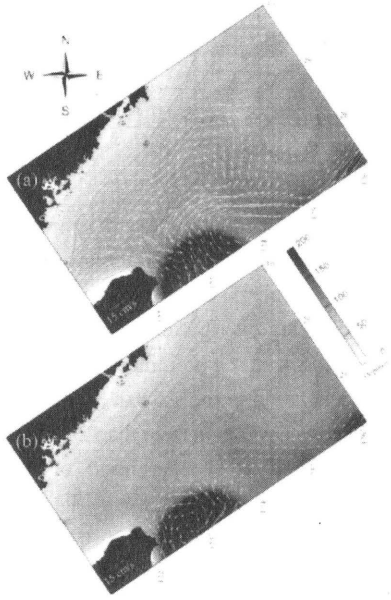

Fig. 3 Velocity difference of Case 1 minus case 2a at 50 m depth in (a) February and (b) August in the box area of Fig. 2. Depth is shown by gray color scale, and dotted lines indicate 50 m, 100 m and 200 m isobaths.

As shown in Fig. 3b, however, the summer velocity difference between the results of case 1 and 2a is much smaller than that of winter because of weak summer southerly winds. Even though weak northward anomaly flow is found off northeast of Taiwan in summer, it mostly turns anticlockwise and flows southward along the east coast of Taiwan. Furthermore, the summer transport through the Taiwan Strait for case 2a is nearly same as that calculated from case 1 (Table 2). These results indicate that strong winter wind largely affects the current pattern in the northern shelf and edge of Taiwan.

5. A passive tracer experiment

Results for wind forcing situations provide some indications of the general circulation and the influence of wind on the ECS shelf water. However, the model-predicted hydrographic features do not provide relative contributions of the onshore Kuroshio intrusion and the Taiwan Warm Current to the property of the ECS shelf water. To compare the contributions, a passive tracer experiment is conducted in this section. By the tracer experiments using a local ECS model, Jacobs et al. (2000) and Lee and Matsuno (2007) examined the contributions of the Kuroshio and the Taiwan Warm Current to the ECS environment. However, their local sea models were not considered the effect of wind on the shelf region around Taiwan because the southern boundary which lies over the Taiwan Strait was closed or fixed for the tracers and fluxes. As pointed out in previous section, difference between the wind forcing situations is largest in the Taiwan Strait and northeast of Taiwan during wintertime. Our model can be a solution to the boundary problems in the local sea model since the boundary conditions are far away from the shelf region around Taiwan.

To determine the contribution from the Taiwan Warm Current and Kuroshio to the water property on the ECS shelf, passive tracers were released at the Taiwan Strait and east of Taiwan, respectively, for four model years after spin-up period. The tracers are independent of each other but they move in the same current field in the model interior. The tracer concentration at each location is fixed to 1.0 while those at other boundaries are fixed to zero during tracer calculation. The concentration of tracers is governed by the advection-diffusion equation in the model interior.

5.1 Tracer distributions

Figure 4 compares the tracer distribution from the Taiwan Strait and Kuroshio in the result of case 1. As a response to the seasonal variation of Taiwan Warm Current, the tracer from the Taiwan Strait shows a remarkable seasonal behavior over the ECS shelf. In winter the tracer from the Taiwan Strait is mostly seen from the Taiwan Strait to YS along the 50 m isobath, and small part of the tracer follows along the ECS shelf (Fig. 4a). The tracer from the Taiwan Strait contributes only a small fraction of the winter distribution at the Korea/Tsushima Strait (< 0.3). In summer, however, the tracer is largely dominant along the elongated shelf from the Taiwan to Korea/Tsushima Straits (Fig. 4b). It reaches a maximum of about 0.7 at the Korea/Tsushima Straits.

By contrast, the tracer from the Kuroshio intrudes onto the shelf off northeast of Taiwan and it extends farther northeastward along the ECS shelf region in winter (Fig. 4c). A tracer concentration above 0.6 also continues to the East/Japan Sea after passing through the Korea/Tsushima Straits. In summer, however, the tracer distributed in the shelf region along the inshore side of the Kuroshio almost vanishes and its concentration at the Korea/Tsushima Strait also decreases largely. This is because the increased inflow through the Taiwan Strait during summer provides more water mass to displace and dilute the Kuroshio water in the continental shelf along the inshore side of the Kuroshio.

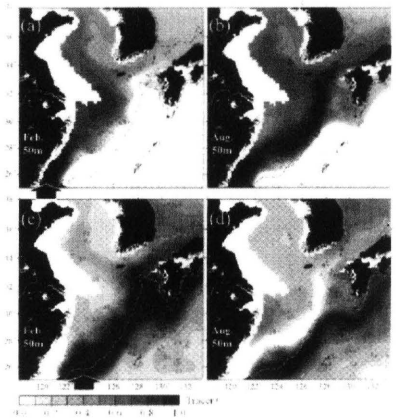

Fig. 4 Monthly averaged distributions of the tracer from (a, b) the Taiwan Strait and (c, d) Kuroshio at 50 m depth in February and August for the result of case 1. Black arrows and dashed line indicate the release location of the tracers and 200 m isobath, respectively.

The seasonal contribution to the ECS shelf water is also shown in the vertical distributions of the tracer from the Kuroshio (Fig. 6). The vertical sections are marked in Fig. 5. For all sections, the tracer is well mixed vertically and its concentration increases gradually from inshore side to offshore side in winter (Fig. 6a, c, e). A tracer concentration above 0.5 is mainly distributed offshore region deeper than 100 m. On the other hand, tracer in the upper and lower layer shows a quite different distribution during summer (Fig. 6b,

d, f). High concentration of the tracer retreats seaward in the upper layer, while it intrudes shoreward in the lower layer compared to that in winter. The offshore retreat in the upper layer is because the Kuroshio water is displaced by the more water mass advected from the Taiwan Strait in summer when the transport through the Taiwan Strait increases substantially. In particular, at the transect B (see Fig. 6d) a shoreward intrusion in the lower layer in summer explains the presence of the Kuroshio water in the offshore area of the Changjiang River mouth shown in right panel of Fig. 4d. This can be explained by the bottom Ekman layer that transports the intruded Kuroshio water northward to the Chinese coastal area, as reported by Jacobs et al. (2000).

The effect of wind forcing on the tracer distribution is presented by differencing the model experiments of case 1 and 2a (Fig. 7). As the summer monsoon winds have little impact on the summer circulation of the ECS (Jacobs et al., 2000; Moon et al., 2009), the difference of summer tracer distribution is much smaller than in winter. In winter a positive concentration of the tracer from the Taiwan Strait is only distributed in the northern YS (Fig. 7a), indicating that the tracer from the Taiwan Strait extends farther northward into the YS due to winter monsoon winds. On the other hand, a negative concentration occupies the elongated continental shelf along the inshore side of the Kuroshio. The area indicated by the negative value is consistent with the area where the concentration difference of the tracer from the Kuroshio is positive as shown in Fig. 7c. The difference of tracer concentration during winter is associated with the decreasing inflow transport through the Taiwan Strait and the intense onshore Kuroshio intrusion due to the strong winter monsoon. These results support the response to the wind forcing revealed by the current fields, as stated in section 4.

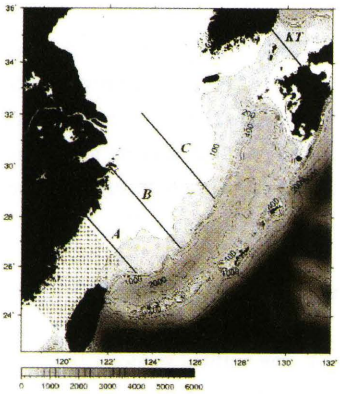

Fig. 5 Transects across which the concentrations are examined in section 5. Circle symbols indicate the grid points where the wind forcing is applied in the Taiwan Strait region for the experiment of case 2b. Depth is shown by gray color scale.

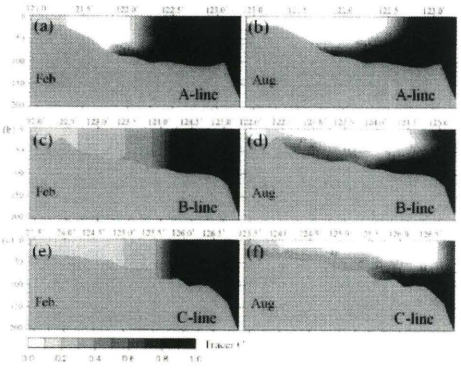

Fig. 6 Monthly averaged vertical distributions of the tracer from the Kuroshio for the result of case 1 at each section in February and August: (a, b) A-line; (c, d) B-line and (e, f) C-line. Contour interval is 0.1.

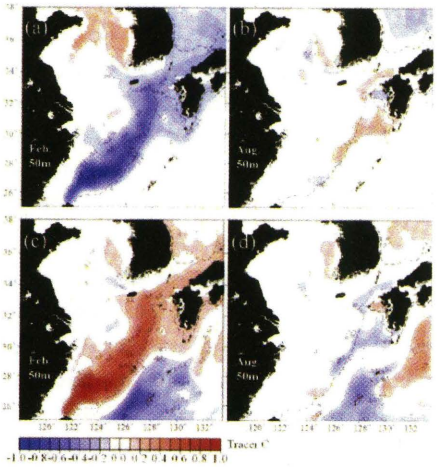

Fig. 7 Same as Fig. 4 except for the difference concentrations of case1 minus case 2a.

5.2 Contribution of the tracers to the ECS shelf water

To quantify and more directly compare the contribution from the tracers to the ECS shelf water, averaged tracer concentrations in each section of Fig. 5 are estimated. As shown in Fig. 8, two time series of the tracers from the Taiwan Strait and Kuroshio show a remarkable seasonal variation in all sections for case 1 (solid lines of Fig. 8). The tracer concentration from the Taiwan Strait reaches its minimum of about 20% in winter and maximum of about 60% in summer for all sections (Fig. 8a, c, e). On the other hand, the tracer from the Kuroshio has an opposite seasonal contribution to that from the Taiwan Strait (Fig. 8b, d, f). The seasonal variability of the tracers on the ECS shelf region is dominant in the upper layer (above 50 m) rather than the

lower layer (not shown).

However, the seasonal variations of the tracer contribution almost disappear when the wind forcing is not applied to the model as presented in dotted lines of Fig. 8. Throughout the year, the contributions from the Taiwan Strait and Kuroshio reach about 55% and 45%, respectively. The seasonal contributions on the ECS shelf from two tracers are direct consequences of the seasonal variation of the Taiwan Warm Current and the onshore Kuroshio intrusion northeast of Taiwan controlled by the strong winter winds. Moreover, a sensitivity experiment on the wind showed a linear response of tracers to the wind strength: when winter winds become stronger, the contribution of the tracer from the Taiwan Strait decreases while that from the Kuroshio increases (not shown). It shows that strong northeasterly wind tends to weaken the Taiwan Warm Current and enhance the intrusion of the Kuroshio warm water, implying that the seasonal variation of the ECS shelf water is substantially controlled by the wind forcing particularly during wintertime.

In general, thermal front is dynamically associated with the circulations of the ECS (Park and Chu, 2006). To support the seasonal variation of the shelf water, we used here thermal front calculated from the observed data set (GDEM) as suggested by Park and Chu (2006). The horizontal temperature gradient is calculated on each data point at the depth of 50 m as follow.

$$|\Delta T(i,t)| = \sqrt{\left(\frac{\partial T(i,t)}{\partial x}\right)^2 + \left(\frac{\partial T(i,t)}{\partial y}\right)^2} \qquad (2)$$

Let $T(i,t)$ be a variable of temperature with (i,t) the spatial and temporal indices. Fig. 9 shows the temperature gradient distributions at the depth of 50 m in (a) February and (b) August from the GDEM data. The regions where temperature gradient is higher than 2°C/100 km are shaded with a contour interval of 1°C/100 km. The criterion of 2°C/100 km is evaluated as the most reasonable value to identify the thermal fronts in the ECS by Park and Chu (2006).

In winter strong thermal front is distributed off northeast of Taiwan and it extends northeastward along the inshore side of the Kuroshio (Fig. 9a). The thermal front is generated between the Kuroshio warm water and the cold water on the shelf. This supports the intruded Kuroshio warm water onto the ECS shelf at the northeast of Taiwan. Meanwhile, in summer the thermal front off northeast of Taiwan shifts seaward and relatively weak thermal front appears along the continental shelf break of the ECS (Fig. 9b). From the thermal front distributions, we can conjecture that the Kuroshio migrates seasonally off northeast of Taiwan, moving shoreward in winter and seaward in summer, implying that the intruded Kuroshio warm water is intensified in winter. Some observation and numerical models also showed an intense onshore Kuroshio intrusion northeast of Taiwan in winter (Sun, 1987; Tang et al., 1999; Guo et al., 2006; Lee and Matsuno, 2007). Also, the presence of strong thermal front around Chinese coast supports the northward extension of the Kuroshio water in summer through the bottom Ekman layer, as suggested by Jacobs et al. (2000).

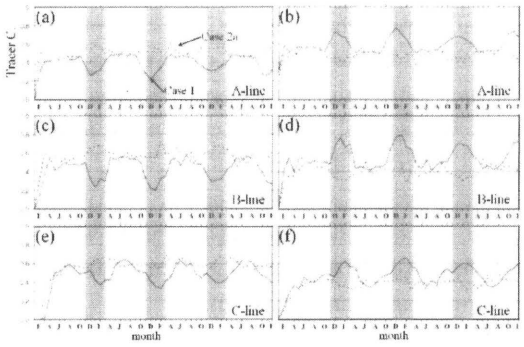

Fig. 8 Time series of mean concentrations of the tracer from (a, c, e) the Taiwan Strait and (b, d, f) Kuroshio in each section for the results of case 1 and case 2a during 4 years for the tracer calculations. Solid and dotted line indicate the results of case 1 and case 2a, respectively. Also stippled bars are marked to emphasize the contribution of the tracers from the Taiwan Strait and Kuroshio in wintertime (from December to March).

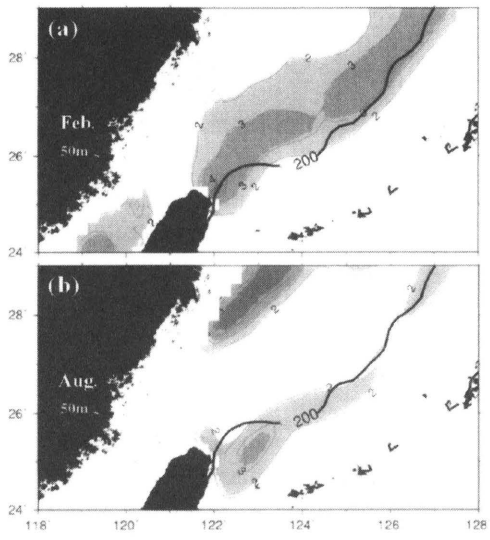

Fig. 9 Temperature gradient distributions at 50 m depth in (a) February and (b) August calculated from the GDEM data. Regions where temperature gradient is higher than 2 °C/100 km are shaded with a contour interval of 1°C/100 km.

6. Discussions

6.1 Origin of the Tsushima Warm Current (TWC)

The onshore Kuroshio intrusion is important from the viewpoint of material transport through the Korea/Tsushima Strait. Fig. 10a shows the time-space plot of the tracer concentration from the Kuroshio at 5 m depth along the KT-line of Fig. 5 during 4 years for the result of case 1. The contribution of the tracer at the Korea/Tsushima Strait shows a remarkable seasonal variation. From winter to spring, the Kuroshio water is dominant in the strait, while it is substantially decreased from summer to autumn. The Kuroshio water in the upper layer during wintertime is almost displaced by the water advected from the Taiwan Strait during summertime (Fig. 10c).

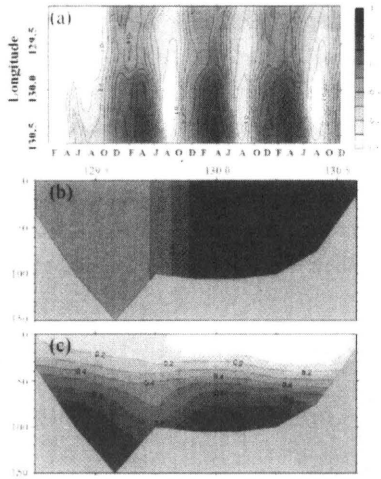

Fig. 10 (a) Time series of mean concentration of the tracer from the Kuroshio at 5 m depth along the KT-line in Fig. 5 for the result of Case 1 during 4 years for the tracer calculation. Vertical distributions of monthly averaged tracer concentration from the Kuroshio along the KT-line in (b) February and (c) August are shown.

Monthly mean tracer transport (= volume transport times tracer concentration) through the Korea/Tsushima Straits are presented in Fig. 11 to estimate on the origin of the material passing through the strait. With wind forcing two time series of the tracer from the Taiwan Strait and Kuroshio show a noticeable seasonal variability. From winter to spring, the tracer transport from the Kuroshio reaches a maximum of about 80 % of the total tracer transport (solid line of Fig. 11a), while that from the Taiwan Strait show a minimum of about 20 % (dotted line of Fig. 11a). From summer to autumn, about 60% of the tracer comes from the Taiwan Strait and the other from the Kuroshio. The annual mean tracer transports from the Taiwan Strait and Kuroshio reach about 40 % and 60 % of total tracer transport, respectively. This estimate agrees well with the result of Guo et al. (2006).

After turning off the wind forcing, however, the seasonal contributions from each tracer almost vanish; about half of the tracer comes from the Kuroshio and the other half from the Taiwan Strait throughout the year (Fig. 11b). This indicates that an opposite seasonal contribution of the tracers to the Tsushima Warm Current primarily depends on the seasonal variation of the Taiwan Warm Current and the onshore Kuroshio intrusion northeast of Taiwan.

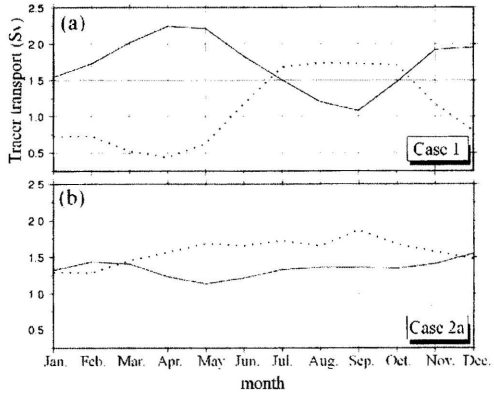

Fig. 11 Monthly mean tracer transport through the Korea/Tsushima Straits from the Taiwan Strait (dotted line) and the Kuroshio (solid line): (a) the result of case 1; (b) case 2a.

6.2 Role of the Taiwan Warm Current on the ECS shelf water

Result between the wind forcing situations (cases 1 and 2a) show an indication that the onshore Kuroshio intrusion northeast of Taiwan is intensified in wintertime when strong northeasterly wind is dominant over the area. As a result, the tracer from the Kuroshio mostly occupies the continental shelf of the ECS during winter. For the Kuroshio onshore flux across the ECS shelf break, Guo et al. (2006) suggested that its seasonal variation is primarily controlled by the Ekman transport across the shelf break induced by northeasterly wind over the ECS shelf, using a vorticity equation to separate the contribution of Ekman transport to the Kuroshio onshore fluxes in the ECS from that relating to density fields. However, even if the vorticity balance provides a contribution of Ekman transport, which is a direct wind-driven transport of seawater, it may be insufficient to explain the seasonal variation of the ECS shelf water because the inflow onto the shelf through the Taiwan Strait is also

the strait (Jan and Chao, 2003; Wang et al., 2003; Lin et al., 2005).

Without wind forcing the transport through the Taiwan Strait is substantially increased in winter and therefore, about half of the water on the shelf region comes from the Taiwan Strait and the other half originates the Kuroshio, as described in Fig. 8. This suggests that the seasonal variability of the ECS shelf water could be controlled by the Taiwan Warm Current rather than the onshore Kuroshio across the shelf break. To examine the role of the Taiwan Warm Current on the ECS shelf water, we conducted an additional experiment, applying the local wind forcing to the Taiwan Strait region only (named case 2b). The seasonal wind forcing is imposed to the model grid points in Fig. 5, but not applied to the other regions. The seasonal transport through the Taiwan Strait in case 2b is nearly the same as the result of case 1 although the winter transport is slightly larger than in case 1 (Table 2). This is one indication that the transport through the Taiwan Strait is primarily driven by a local wind over the Taiwan Strait, not over the entire ECS.

Table 2 Monthly mean volume transports (Sv, 1Sv ≡ $10^6 m^3 s^{-1}$) through the Taiwan Strait for the three model experiments of Case 1, Case 2a and Case 2b.

	Feb.	Apr.	Jun.	Aug.	Oct.	Dec.
Case1	1.1	2.3	2.6	2.4	0.7	0.4
Case2a	2.4	2.4	2.4	2.3	2.4	2.3
Case2b	1.5	2.0	2.4	2.3	1.1	0.7

Fig. 12 shows the monthly averaged concentration of the tracer from the Kuroshio in each section for the three experiments. An interesting result is that in case 2b the tracer contribution to the ECS shelf water shows almost the same seasonal variation with that of case 1 and its seasonal contribution occurs in all sections. For the experiment of case 2b, wind forcing is only applied in the Taiwan Strait region, implying that there is no Ekman transport across the shelf break of the ECS. In other word, the ECS shelf water originating from the Kuroshio has a remarkable seasonal variation regardless of Ekman transport across the shelf break. The seasonal variation of the shelf water may depend on changes in the strength of the Taiwan Warm Current, which appear to block the Kuroshio water on the shelf and thus prevent the onshore Kuroshio intrusion northeast of Taiwan in upper layer. Moreover, an opposite experiment to case 2b, turning off the wind forcing only Taiwan Strait region, showed a similar result to case 2a (not shown). It also support that the Taiwan Warm Current did markedly impact the seasonal variation of the ECS shelf water. Comparison between comparative experiments suggests that the seasonal variation of the ECS shelf water could be determined by the strength of the Taiwan Warm Current driven by the wind forcing over the Taiwan Strait.

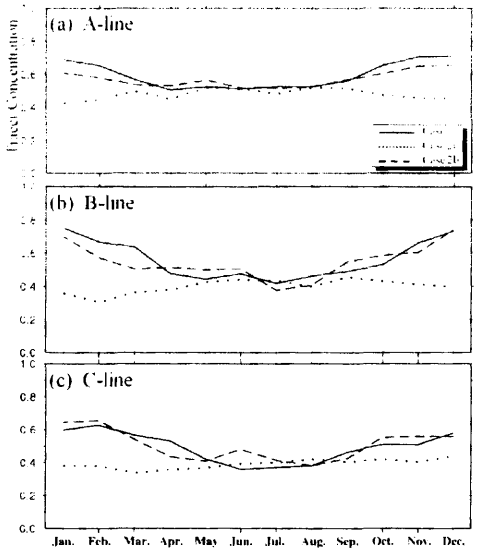

Fig. 12 Monthly averaged concentrations of the tracer from the Kuroshio in each section for the results of Case 1 (solid line), Case 2a (dotted line) and Case 2b (dashed line). The tracer concentration is averaged for last 3 years for the tracer calculation.

7. Summary

This study investigates the influence of wind forcing on the seasonal variation of the ECS shelf water. Since the ECS environment is strongly affected by the inflows through the Taiwan Strait and Kuroshio as the open boundary conditions, we here use a northwestern Pacific circulation model to diagnose the wind effect associated with the boundaries. The model is initialized with climatological temperature and salinity obtained from the GDEM. The model was spun up with all forces for 24 model years. Basically, two numerical experiments were run for additional 4 years after 24 years of spin-up: one with wind forcing and one without. Tracer experiments are computed in order to examine the contribution of the Taiwan Warm Current water and the Kuroshio water to the ECS environment. To discuss the role of the Taiwan Warm Current on the ECS shelf water, we conducted an additional experiment, only applying the seasonal wind forcing to the Taiwan Strait region.

Comparison between the wind and no-wind cases shows that strong northeasterly wind forcing in winter significantly weakens the Taiwan Warm Current entering the ECS shelf through the Taiwan Strait and plays a role in intensifying the onshore Kuroshio intrusion northeast of Taiwan. However, the summer monsoon winds have small amplitude and

therefore have little impact on the ECS circulation. As a result, the transport through the Taiwan Strait is considerably decreased in winter and its seasonality is remarkable. On the other hand, the onshore Kuroshio intrusion northeast of Taiwan is intensified in winter when the Taiwan Warm Current becomes weaker by the strong northeasterly wind.

The results for inserting two separate tracers into the model support the seasonality of the ECS shelf revealed by the current fields. In winter the tracer from the Taiwan Strait is mostly seen from the Taiwan Strait to YS along the 50 m isobath and a small portion of the tracer distributes along the ECS shelf. The tracer contributes only a small fraction of the winter distribution in the Korea/Tsushima Strait, but it prevails in summer from the Taiwan to Korea/Tsushima Straits along the continental shelf. On the other hand, the tracer from the Kuroshio shows an opposite seasonal variation to that from the Taiwan Strait. In winter the tracer concentration from the Kuroshio increases off northeast of Taiwan and along the continental shelf of the ECS, while it almost vanishes in the continental shelf along the inshore side of the Kuroshio. As a result, the tracer transport through the Korea/Tsushima Strait has a remarkable seasonal variation. From winter to spring, the transport from the Kuroshio increases up to about 80% of total tracer transport, while that from the Taiwan Strait decreases to about 20% of total tracer transport. From summer to autumn, about 60% of total tracer transport comes from the Taiwan Strait and the other from the Kuroshio.

However, without wind forcing the seasonal contributions from each tracer almost disappear. About half of the tracer comes from the Kuroshio and the other half from the Taiwan Strait throughout the year. Consequently, the seasonal contributions from the two tracers to the ECS shelf water are direct consequences of the seasonal variation of the Taiwan Warm Current and the onshore Kuroshio intrusion northeast of Taiwan. Moreover, the ECS shelf water seasonally changes regardless of Ekman transport across the ECS shelf break according to an additional experiment, only applying the seasonal wind forcing in the Taiwan Strait region. This result suggests that the seasonal variation of the shelf water could be determined by changes in the strength of the Taiwan Warm Current driven by the wind forcing over the Taiwan Strait, which appear to block the Kuroshio water on the shelf and thus prevent the onshore Kuroshio intrusion northeast of Taiwan.

Acknowledgements

I wish to express my gratitude to my supervisor, Professor Jong-Hwan Yoon for his physical insight and kind encouragement during this study.

References

1) Adcroft, A., C. Hill, and J. Marshall, 1997. Representation of topography by shaved cells in a height coordinate ocean model. *Mon. Wea. Rev.*, 125, 2293-2315.
2) Barnier, B., L. Siefridt, and P. Marchesiello, 1995. Thermal forcing for a global ocean circulation model using a three-year climatology of ECMWF analyses. *J. Mar. Sys.*, 6, 363-380.
3) Chang, P. H. and A. Isobe, 2003. A numerical study on the Changjiang Diluted Water in the Yellow and East China Seas. *J. Geophys. Res.*, 108(C9), 3299, doi:10.1029/ 2002JC001749.2003.
4) Chern, C. S. and J. Wang, 1992. The influence of Taiwan Strait waters on the circulation of the southern East China Sea. *La Mer*, 30,223-228.
5) Choi, B. H., K. O. Kim, and H. M. Eum, 2002. Digital bathymetric and topographic data for neighboring seas of Korea. *J. Korean Soc. Coastal Ocean Eng.*, 14, 41-50 (in Korean with English abstract).
6) Da Silva, A. M., Young, C. D., Levitus, S., Atlas of Surface Marine Data, 1994. Vol. 1, Algorithms and Procedures. NOAA Atlas NESDIS 6, U. S. Department of Commerce, NOAA, NESDIS, USA, 74 pp.
7) Guo, X., Y. Miyazawa and T. Yamagata, 2006. The Kuroshio onshore intrusion along the shelf break of the East China Sea: the origin of the Tsushima Warm Current. *J. Phys. Oceangr.* 36, 2205-2231.
8) Ishizaki, H. and T. Motoi, 1999. Reevaluation of the Takano-Oonishi scheme for momentum advection on bottom relief in ocean models. *J. Atmos. Ocean. Tech.*, 16, 1994-2010.
9) Isobe, A. and R. C. Beardsley, 2006. An estimate of the cross-frontal transport at the shelf break of the East China Sea with the Finite Volume Coastal Ocean Model. *J. Geophys. Res.* 111, C03012, doi: 10.1029/2005 JC003290.
10) Jacobs, G. A., H. B. Hur, and S. K. Riedlinger, 2000. Yellow and East China Seas response to winds and currents. *J. Geophys. Res.*, 105, 21947-21968.
11) Jan, S., Wang, J. Chern, C.-S. and S.-Y., Chao, 2002. Seasonal variation of the circulation in the Taiwan Strait. *J.Mar. Sys.* 35, 249-268.
12) Jan, S. and S.-Y., Chao, 2003. Seasonal variation of volume transport in the major inflow region of the Taiwan Strait: the Penghu Channel. *Deep-Sea Research II,* 50, 1117-1126.
13) Katoh, O., K. Morinaga and N. Nakagawa, 2000. Current distributions in the southern East China Sea in summer. *J. Geophys. Res.,105, No.* C4, 8565-8573.

14) Kim, K., H.K. Rho and S.H. Lee, 1991. Water Masses and Circulation around Cheju-Do in summer. *J. Oceanog. Soc. Korea*, 26(3): 262-277.

15) Lee, H. C., 1996. A numerical simulation for the water masses and circulations of the Yellow Sea and the East China Sea. Ph. D. Thesis, Kyushu University.

16) Lee J.-S. and T. Matsuno, 2007. Intrusion of Kuroshio water onto the continental shelf of the East China Sea. *J. Oceangr.*, 63, 309-325.

17) Lee, S.-H. and R. C. Beardsley, 1999. Influence of stratification on residual tidal currents in the Yellow Sea. *J. Geophys. Res.*,104(C7),15679-15701

18) Lin, S. F., T. Y. Tang, S. Jan and C.-J. Chen, 2005. Taiwan Strait current in winter. *Cont. Shelf Res.*, 25, 1023-1042.

19) Liu, K.-K., G.-C. Gong, C.-Z. Shyu, S.-C. Pai, C.-L. Wei, and S.-Y. Chao, 1992. Response of Kuroshio upwelling to the onset of the northeast monsoon in the sea north of Taiwan: Observations and a numerical simulation. *J. Geophy. Res.*, 97, No. C8,12511-1226.

20) Moon, J.-H., N. Hirose, J.-H. Yoon and I.-C. Pang, 2008. Effect of the along-strait wind on the volume transport through the Tsushima/Korea Strait in September. *J. Oceanogr.*, in press

21) Noh, Y., C. J. Jang, T. Yamakata, P. C. Chu and C.-H. Kim, 2002. Simulation of more realistic upper-ocean processes from an OGCM with a new ocean mixed layer model. *J. Phys. Oceanogr,* 32, 1284-1307.

22) Park, S. Y. and P. C. Chu, 2006. Thermal and Haline Fronts in the Yellow/East China Seas: Surface and Subsurface Seasonality Comparison. *J. Oceanogr.*, 62, 617-638.

23) Park, Y. H., 1986. A simple theoretical model for the upwind flow in the southern Yellow Sea. *J. Oceanol. Soc. Korea*, 21, 203-210.

24) Qiu, B., and N. Imasato, 1990. A numerical study on the formation of the Kuroshio countercurrent and the Kuroshio branch current in the East China Sea. *Cont. Shelf Res.*, 10, 165-184.

25) Sun, X., 1987. Analysis of the surface path of the Kuroshio in the East China Sea. In *Essasy on Investigation of Kuroshio*, ed. by X. Sun, China Ocean Press, Beijing, 1-14

26) Tang, T. Y., Y. Hsueh, Y. J. Yang and J. C. Ma, 1999. Continental slope flow northeast of Taiwan. *J. Phys. Oceanog.*, 29, 1353-1362.

27) Takano, K., 1978. Influences of ridges on deep and bottom flows. *Oceanography as Environmental Science, S. Horibe, Ed., Tokyo University Press.* Tokyo, 27-44. (in Japanese)

28) Wang, Y. H., S. Jan and D. P. Wang, 2003. Transports and tidal current estimates in the Taiwan Strait from the shipboard ADCP observations (1999-2001). *Estuarine, Coastal and Shelf Sci.*, 57, 193-199.

29) Webb, D. J., B. A. de Cuevas C. S. Richmond, 1998. Improved advection schemes for ocean models. *J. Atmos. Ocean. Tech.*, 15, 1171-1187.

30) Yanagi, T. and S. Takahashi, 1993. Seasonal variation of circulations in the East China Sea and the Yellow Sea. *J. Oceangr.*, 49, 503-520.

31) You, S. H. and J. H. Yoon, 2004. Modeling of the Ryukyu current along the Pacific side of the Ryukyu Island. *Pacific Oceanogr.*, 2, 44-51.

32) Youn, Y. H., Y. Park, and J. H. Bong, 1991. Enlightment of the Characteristics of the Yellow Sea Bottom Cold Water and its southward Extension. *J. Korean Earth Science Society,* Vol. 12(1), 25-37.